Structural Engineering and Mechanics, Vol. 33, No. 1 (2009) 1-14
DOI: http://dx.doi.org/10.12989/sem.2009.33.1.001

Experimental and numerical verification of hydraulic displacement amplification damping system

Tracy Sau-Kwai Chung† and Eddie Siu-Shu Lam‡

Department of Civil and Structural Engineering, Hong Kong Polytechnic University, Hung Hum, Kowloon, Hong Kong

Bo Wu‡†

Department of Civil Engineering, South China University of Technology, Guangzhou, China

You-Lin Xu‡‡

Department of Civil and Structural Engineering, Hong Kong Polytechnic University, Hung Hum, Kowloon, Hong Kong

(Received February 22, 2007, Accepted July 24, 2009)

Abstract. Hong Kong is now recognized as an area of moderate seismic hazard, but most of the buildings have been designed with no seismic provision. It is of great significance to develop effective and practical measures to retrofit existing buildings against moderate seismic attacks. Researches show that beam-column joints are critical structural elements to be retrofitted for seismic resistance for reinforced concrete frame structures. This paper explores the possibility of using a Hydraulic Displacement Amplification Damping System (HDADS), which can be easily installed at the exterior of beam-column joints, to prevent structural damage against moderate seismic attacks. A series of shaking table tests were carried out with a 1/3 prototype steel frame have been carried out to assess the performance of the HDADS. A Numerical model representing the HDADS is developed. It is also used in numerical simulation of the shaking table tests. The numerical model of the HDADS and the numerical simulation of the shaking table tests are verified by experimental results.

Keywords: viscous fluid damper; displacement amplification; retrofitting; beam-column joint; shaking table test.

1. Introduction

Hong Kong is no longer recognized as having immunity against earthquake. In fact, the city is now recognized as an area of moderate seismic hazard (GB50011-2001, Lee *et al.* 1996). Before the

† Ph.D. Candidate, E-mail: cse.tracy.skchung@polyu.edu.hk
‡ Associate Professor, E-mail: cesslam@polyu.edu.hk
‡† Professor, E-mail: bowu@scut.edu.cn
‡‡ Chair Professor, E-mail: ceylxu@polyu.edu.hk

enforcement of the Code of Practice for Structural Use of Concrete (2004) in 2005, buildings in Hong Kong were designed without seismic provision (Lam and Xu 2002). The 1989 Newcastle earthquake has well demonstrated the effect of a moderate earthquake on a city without seismic provision. Jensen (2000) reported that this magnitude 5.6 earthquake caused more than AU$2 billion of property damage and took 13 lives. This earthquake is a typical example of how an intra-plate earthquake with moderate magnitude can cause loss of life and substantial damage if it occurs close to a populated city with the infrastructures and buildings designed without seismic provisions. As Hong Kong is one of the important financial centers and densely populated cities in the world, any interruption to critical facilities and business operation due to moderate earthquake attack may have serious social and economical consequences. The deficiency in the seismic resistance of buildings in Hong Kong requires imminent attention and retrofitting existing buildings against moderate seismic attacks is needed (Lam and Xu 2002).

Reinforced concrete moment frame is a common structural form in low-rise buildings of less than 10 storeys in Hong Kong. Potential weakness in the local beam-column joints may lead to the formation of a brittle soft story or column side-sway mechanism when subjected to moderate seismic action (Booth 1994). Behavior of un-reinforced and lightly reinforced beam-column joints were studied (Dhakal and Pan 2005). Severe degradation in stiffness and bonding at the joint panel was observed.

Traditionally, beam-column joints are retrofitted by improving the confining properties of concrete, such as using Fiber Reinforced Polymer. This method involves demolition of nonstructural elements, affects decoration and takes longer time to complete as compared with adding energy dissipating devices. The occupants will be seriously affected and alternative methods should be considered. Over the years, different types of energy dissipating devices aiming at improving earthquake response and damage control of buildings have been developed. Such devices include, just to name a few, hysteresis dampers (Skinner *et al.* 1975), tapered steel energy dissipaters (Taylor 1978), base-isolation (Robinson and Cousins 1987), etc. In considering the remoteness of seismic risk in areas with moderate seismicity, the use of passive dampers is both viable and economical.

Viscous fluid dampers were firstly developed for military purposes. In recent years, they were incorporated into a large number of civil engineering structures (Constantinou 1994, Tsopelas and Constantinou 1995). They have been shown to be an effective energy dissipation device for structures against earthquake (Shen and Soong 1996, Soong and Spencer 2002) and have also been proven thoroughly to be reliable and robust through decades of Cold War usage (Taylor and Duflot 2003). Lee and Taylor (2001) indicated that response of viscous fluid dampers essentially out of phase with structural shear stresses, and viscous fluid dampers have the capability to reduce both shear stress and deflections in a structure. This feature may prevent introducing additional shear force in the retrofitted columns.

In general, allowable stresses of reinforced concrete are smaller than those of steel. Reinforced concrete structures require larger size elements when comparing with steel structures. Therefore reinforced concrete structures are relatively stiff. As far as moderate seismicity is concerned, deformation of the structures will be small and this may adversely affect the performance of passive dampers. Lever mechanisms and gear mechanism have been suggested to improve passive energy dissipation by amplifying the displacement received by the damping unit (Ribakov *et al.* 2000, Berton 2001, Ribakov and Dancyoier 2006). Ribakov and Reinhorn (2003) studied the influence of flexibility of lever arm system on the efficiency of the amplification. Berton and Bolander (2004) demonstrated the effectiveness in applying amplification to viscous fluid damper.

Considering the limited space in building and moderate seismicity as well as providing alternative displacement amplification for engineers, a Hydraulic Displacement Amplification Damping System (HDADS) was introduced (Chung and Lam 2004a). The HDADS comprises 2 viscous fluid dampers and a displacement amplification system. It can be installed at the exterior of a beam-column joint. Efficiency of the HDADS was assessed through testing a 1/3 scale, 2 stories prototype steel frame on a shaking table. A numerical model representing the HDADS was developed to numerically simulate responses of the 1/3 scale prototype steel frame when subjected to earthquake action. The numerical simulation results were compared with those of the shaking table tests.

2. HDADS

The HDADS comprises a hydraulic displacement amplification system and two viscous fluid dampers, as shown in Fig. 1. The hydraulic displacement amplification system is used to improve the performance of the viscous fluid dampers. It comprises one large and two small bore size hydraulic cylinders. The large bore size cylinder is attached to a beam-column joint, via pinned connections, to perceive the deformation, as shown in Fig. 2. The hydraulic cylinders filled with TELLUS 37 hydraulic oil are connected by 6 mm diameter high pressure pipes. Due to the difference in the cross sectional areas of the hydraulic cylinders, structural deformation perceived by the large bore size hydraulic cylinder is amplified. Details of the hydraulic cylinders are summarized in Table 1. The two viscous fluid dampers are hydraulic dampers type HB-15-100-AA-P manufactured by ACE Controls Inc. The viscous fluid dampers are connected to the small bore size cylinders, to receive the amplified deformation and to dissipate energy. Damping properties of the HDADS can be adjusted by using viscous fluid dampers with specific properties to suit specific damping requirements.

In order to appraise the stability and reliability of the HDADS and to quantify its characteristics related to its performance, the HDADS was subjected to cyclic displacements at different frequencies using a MTS testing machine. Table 2 shows the amplification factor. The amplification

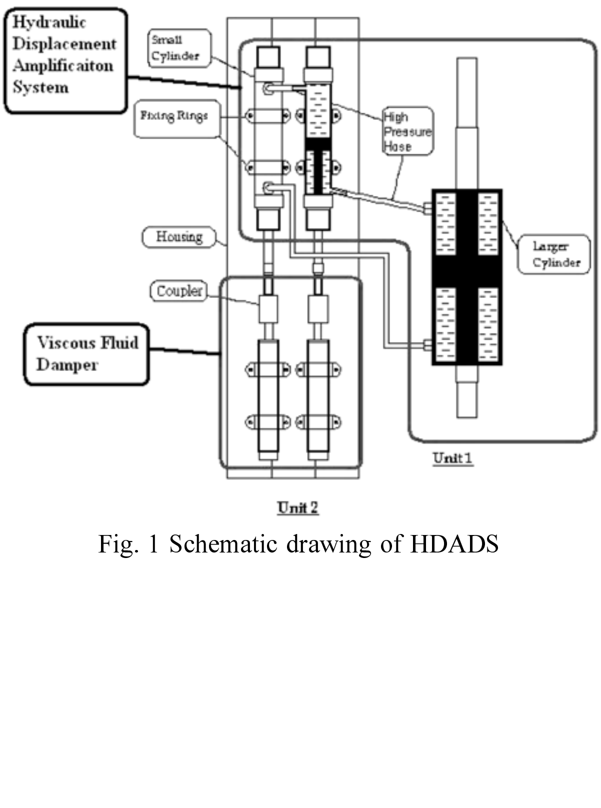

Fig. 1 Schematic drawing of HDADS

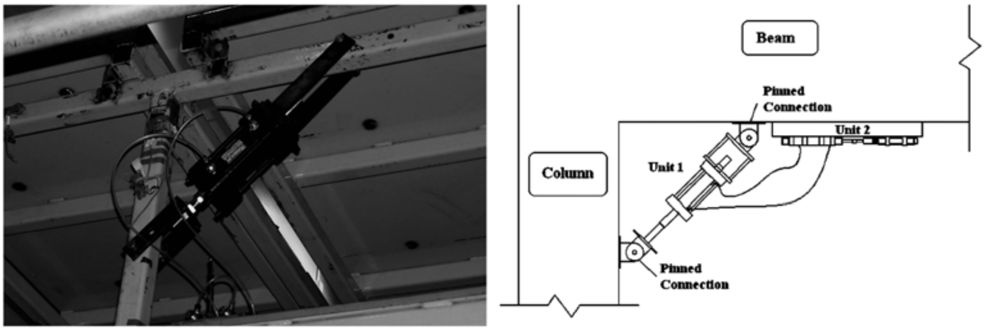

(a) HDADS installed in the prototype steel frame

(b) HDADS installation in beam-column joint

Fig. 2 Installations of the HDADS

Table 1 Parameters of hydraulic cylinders

	Large Bore Size Cylinder (HOD 80-50)	Small Bore Size Cylinder (ROB 20-75)
Bore Diameter (mm)	80	20
Stroke Dia (mm)	40	12
Internal Cross Section Area (mm^2)	3770	201
Area Ratio	18.75	

Table 2 HDADS amplification factor experimental results

Sinusoidal Input Frequency	Amplification factor*	
	Sinusoidal input maximum amplitude	
	1.3 mm	2.0 mm
0.2 hz	5.03	9.90
0.3 hz	5.79	10.68
0.5 hz	7.27	11.40
1 hz	7.47	10.44
2 hz	5.26	7.29
3 hz	4.06	5.53
4 hz	3.44	4.51

*Note: Amplification factor = $\frac{\text{Max stroke distance of small bore size cylinder}}{\text{Max stroke distance of large bore size cylinder}}$

factor is found to be dependant both on frequency and magnitude of the displacement input. This is probably due to possible loss of pressure inside the hydraulic system as the hydraulic oil is not incompressible and the high pressure pipes deform under pressure. The amplification factor is larger at low frequency range (0.2 Hz to 1 Hz). From 1 Hz to 6 Hz, amplification factor decreases with increasing input frequency. At frequency equals to or below 2 Hz, the amplification factor is optimum.

As far as the magnitude of the displacement inputs is concerned, the amplification factor improves in larger displacement input. The reason could be due to the initiating force of motions of hydraulic cylinders, and the frictional force between pistons and internal walls of cylinders. In considering cases with larger displacement input, the ratio of displacement used in initiating motions to that used in moving pistons of cylinders is relatively smaller than that of cases with smaller displacement input.

Fig. 3 shows the hysteretic loops of the HDADS obtained from the experiments. The HDADS contains frictional and viscoelastic properties to provide both damping and stiffness to a structure. Viscoelastic properties of the HDADS are dominant at high frequencies but recessive at low frequencies. Therefore, the hysteretic loops of the HDADS have different shapes at different frequency. Properties of HDADS at frequencies equal to or below 0.5 Hz are similar to a friction damper plus a spring. It behaves similar to a viscoelastic damper at frequencies equal to or higher than 1 Hz. As shown in Fig. 3, the maximum axial force needed to push the HDADS into motion is 9 kN (at 2 Hz). As far as moderate seismicity is concerned, any additional bending moment and/or shear force yielded to the beam and column will be nominal.

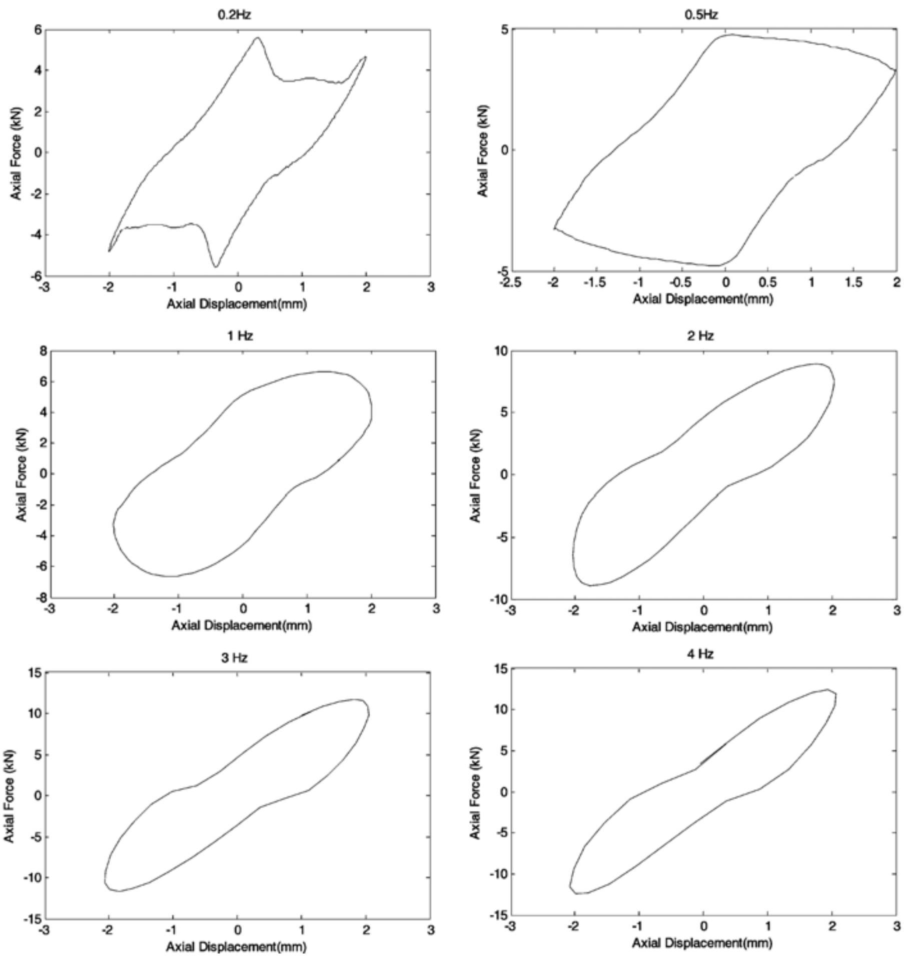

Fig. 3 The HDADS hysteretic loops with a 2 mm sinusoidal displacement input

3. Shaking table test

To quantify the performance of the HDADS, shaking table tests were carried out on a 1/3 prototype steel frame. The prototype steel frame comprises of 2 bays, 2.4 m × 2.0 m in plane, and a total height of 2 m (i.e., 1 m height per storey). All beams and columns of the prototype steel frame are made of 70 × 70 × 5 mm Square Hollow Sections of Grade 43A steel to BS 4360. Table 3 summarizes basic parameters of the steel frame. Within each bay, all members are welded by 4 mm fillet welds all round. The two bays are connected by bolts and nuts. Young's Modulus and Elastic Modulus of the steel section are determined by carrying out tensile tests and two-points loading tests, and are 203.6 MPa and 22880 mm^3 respectively.

Fig. 4 shows the prototype steel frame. For the with HDADS case, 2 sets of HDADS are respectively installed at the middle beam-column joints of the bays at the 2nd floor as shown in Fig. 4(b). Fig. 5 shows the schematic drawing of testing arrangement. 4 tons of artificial masses are placed evenly on the floors to simulate the floor loadings. 50 strain gauges are installed at critical locations such as at the ends of beams, top and bottom of columns, etc. All strain gauges are installed at both sides of structural elements so that bending moment of the section can be determined. 5 accelerometers (Brüel & Kjær Type 4382) are used to monitor the horizontal accelerations of the floors, 2 at the 2nd floor, 2 at the 1st floor and 1 at G/F. 2 Laser Transducers (KEYENCE LK-503) are used to monitor the horizontal translation at the 1st floor and the 2nd floor floor. Accelerations, horizontal floor translations and strain data are recorded at 0.005 second intervals. Natural frequencies of the steel frame with and without HDADS are assessed by carrying out white noise excitations. Table 4 summarizes the modal frequencies and the modal damping ratios of the prototype steel frame. The results have shown that HDADS increases the first natural frequency of the steel frame by about 0.1 Hz, due to some increase in the stiffness as the joints are stiffened by HDADS.

Earthquake excitations including Altadena (N-S), Hollister (N-S), Elcentro (N-S) and Corralitos

Table 3 Parameters of steel frame structure

Dimension	2 Bays, 2 Floors
Floor Height	1.0 m
Bay Width	1.2 m
Mass on Each Loading Slab	1 kNs/m^2 (1 ton)
Lump Mass on centre of each beam	0.5 kNs/m^2
Structural Steel Members: All Steel Section to be 70 × 70 × 5 mm SHS, at 10.1 kg/m (According to Section Table)	
Area	12.9 cm^2
Elastic Modulus, Z	25.7 cm^3
Plastic Modulus, S	31.2 cm^3
Young Modulus, E	1.999×10e8 kN/m^2
Load carrying capacity is of 70 × 70 × 5 mm SHS	
Axial Capacity	322.5 kN
Moment Capacity	7.079 kNm
Shear Capacity (kN)	106.4 kN

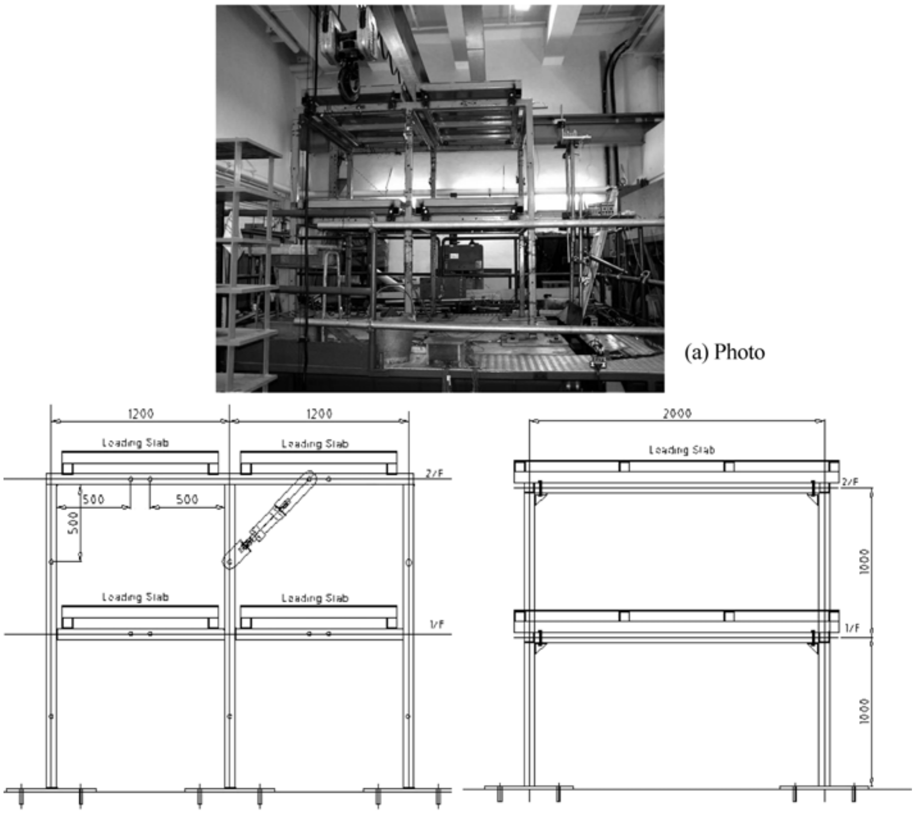

(a) Photo

(b) Elevation in longitudinal direction (c) Elevation in transverse direction

Fig. 4 Prototype steel frame

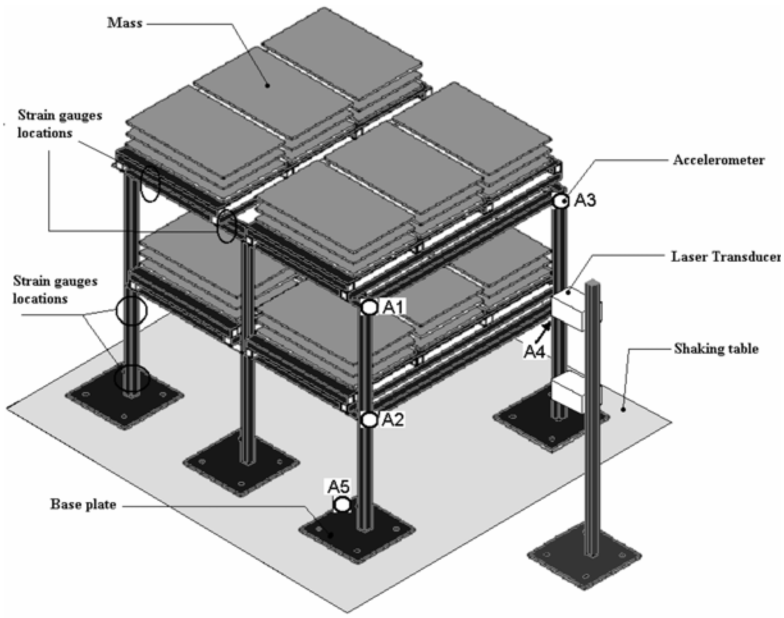

Fig. 5 Schematic drawing of testing arrangement

Table 4 Dynamic properties of steel frame

Steel Frame Condition	1st Mode		2nd Mode	
	Frequency (Hz)	Damping Ratio	Frequency (Hz)	Damping Ratio
With HDADS	4.248	0.02748	13.916	0.00162
Without HDADS	4.150	0.06531	14.522	0.01269

Table 5 Summary of equivalent viscous damping and stiffness of HDADS

Frequency (Hz)	Energy Dissipated per cycle, U (kNmm)	Equivalent Viscous Damping C_{eq} (kNs/mm)	Stiffness, K_{eq} (kN/mm)
0.2	15.77	0.997	2.324
0.3	17.16	0.722	2.012
0.5	20.76	0.524	1.657
1	28.11	0.351	2.069
2	28.20	0.172	3.604
3	34.30	0.136	4.765
4	30.99	0.091	5.806
5	25.29	0.058	5.846
6	25.12	0.047	6.276

Table 6 Summary of interstory drift at the 2nd floor due to earthquake excitation

Peak Ground Acceleration (G)	Earthquake	Shaking Table Test 2nd Floor Interstory Drift (mm)			Numerical Simulation 2nd Floor Interstory Drift (mm)		
		No Damper	With Damper	Reduction (mm)	No Damper	With Damper	Reduction (mm)
0.05	Altadena	1.17	0.91	0.26	1.25	1.04	0.21
0.07	Altadena	1.89	1.23	0.65	1.75	1.46	0.29
0.09	Altadena	2.39	1.61	0.78	2.25	1.88	0.37
0.05	Corralit	1.18	0.90	0.28	1.02	0.87	0.15
0.07	Corralit	1.54	1.49	0.05	1.43	1.22	0.21
0.09	Corralit	1.78	1.57	0.21	1.83	1.56	0.27
0.05	Elcentro	0.77	0.57	0.20	0.91	0.71	0.2
0.07	Elcentro	1.08	1.01	0.07	1.26	1.00	0.26
0.09	Elcentro	1.76	1.32	0.44	1.63	1.29	0.34
0.05	Holliste	0.63	0.52	0.12	0.65	0.52	0.13
0.07	Holliste	0.82	0.61	0.21	0.91	0.73	0.18
0.09	Holliste	1.16	0.90	0.26	1.16	0.94	0.22

(N-S) are considered. According to the similitude law (Harris and Sabnis 1999), the scale factor in the time domain for the seismic records is $1/\sqrt{3}$. Table 6 summarizes the maximum interstory drift at the 2nd floor when subjected to the earthquake records. In all the cases, the addition of HDADS reduces interstory drifts at the 2nd floor and the reduction is in the range of 15 to 25 percents.

Table 7 Summary of interstory drift at the 2nd floor subjected to sinusoidal excitation

Frequency of Sinusoidal Excitation (Hz)	Peak Ground Acceleration (G)	Shaking Table Test			Numerical Simulation		
		No Damper, Interstory Drift at the 2nd floor (mm)	With Damper, Interstory Drift at the 2nd floor (mm)	Reduction (mm)	No Damper, Interstory Drift at the 2nd floor (mm)	With Damper, Interstory Drift at the 2nd floor (mm)	Reduction (mm)
1	0.1	0.77	0.59	0.19	0.79	0.73	0.06
1	0.15	1.11	0.87	0.24	1.19	1.08	0.11
1	0.25	1.83	1.47	0.35	1.98	1.81	0.17
1.5	0.1	0.84	0.69	0.15	0.88	0.81	0.07
1.5	0.15	1.29	1.13	0.16	1.33	1.21	0.12
1.5	0.25	2.19	1.94	0.24	2.22	2.02	0.20
2	0.1	0.91	0.78	0.13	0.96	0.87	0.09
2	0.15	1.28	1.21	0.07	1.44	1.29	0.15
2	0.25	2.12	1.93	0.18	2.40	2.16	0.24

Table 8 Summary of acceleration at the 2nd floor subjected to sinusoidal excitation

Frequency of Sinusoidal Excitation (Hz)	Peak Ground Acceleration (G)	No Damper, acceleration (mm/s^2)	With Damper, acceleration (mm/s^2)	Reduction (mm/s^2)
1	0.1	1.06	1.07	0.00
1	0.15	1.59	1.54	0.04
1	0.25	2.70	2.74	−0.04
1.5	0.1	1.20	1.19	0.01
1.5	0.15	1.82	1.84	−0.02
1.5	0.25	3.42	3.20	0.22
2	0.1	1.41	1.24	0.17
2	0.15	1.99	1.88	0.11
2	0.25	3.49	3.30	0.19

Sinusoidal excitations with frequency range from 1 to 2 Hz are also considered. The results show that the reduction in interstory drift increases when the magnitude of excitation is increased. Tables 7 and 8 summarize the maximum interstory drift and floor acceleration when subjected to sinusoidal excitation with frequency ranged from 1 to 2 Hz and acceleration between 0.10 and 0.25 g. The HDADS can reduce interstory drift at the 2nd floor by about 10 to 20% and floor acceleration at the 2nd floor by up to about 10%. HDADS can be a plausible way to retrofit existing beam-column joints for moderate seismic earthquake.

4. Numerical model of HDADS

A numerical model representing the HDADS is developed. Properties of the HDADS obtained from the experimental hysteresis tests are analyzed and a numerical model is proposed based on an equivalent damping coefficient concept (Steidel 1989). Hysteretic behavior of the HDADS is found to be similar to a viscoelastic damper, as shown in Fig. 3. The hysteretic properties are estimated based on two criteria. They are equal energy dissipated per cycle and equal equivalent stiffness, as shown in Fig. 6.

$$F = K_{eq} \times x + C_{eq} \times v \tag{1}$$

$$C_{eq} = \frac{\Delta U}{\pi \omega X_{\max}^2} \tag{2}$$

$$K_{eq} = \frac{F_P}{X_{\max}} \tag{3}$$

Where F : Resistance force of HDADS;
K_{eq} : Equivalent stiffness;
C_{eq} : Equivalent viscous damping;
x : Piston deformation of HDADS larger cylinder;
v : Piston velocity of HDADS larger cylinder;
F_P : Resistance force of HDADS when x equals to $X_{\max}$;

Resistance force of the HDADS model can be obtained from Eq. (1). Graphical illustrations of the

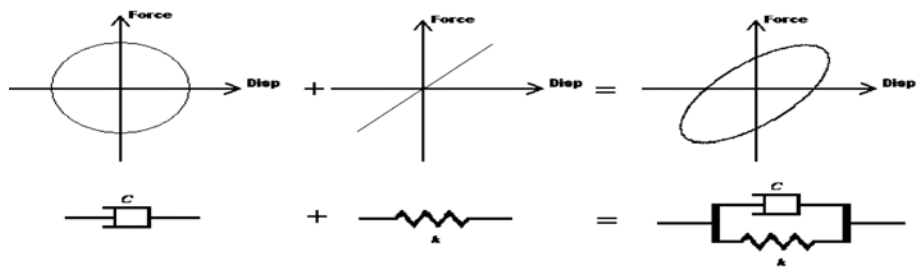

Fig. 6 Graphical illustration of HDADS numerical model

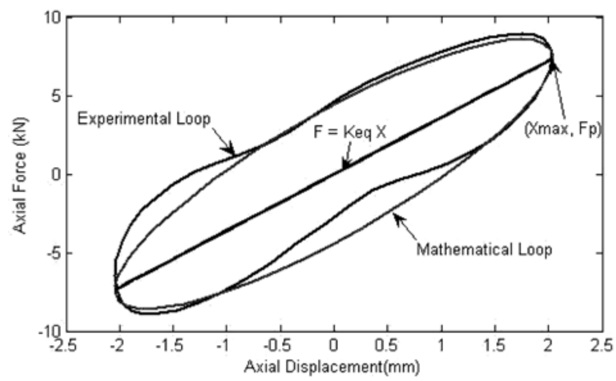

Fig. 7 Experimental and numerical hysteresis loop of HDADS with a 3 Hz, 2 mm maximum amplitude sinusoidal displacement input

HDADS numerical model are shown Fig. 6. The equivalent viscous damping can be determined from Eq. (2), where ΔU, ω, and $X_{\max}$ are energy dissipated per cycle, angular velocity, and maximum amplitude of sinusoidal displacement input respectively. Equivalent stiffness, K_{eq}, can be determined from Eq. (3). When maximum displacement occurs, velocity is equal to zero. Fig. 7 shows the hysteresis loops obtained from the experiments and by applying Eq. (1) (Chung and Lam 2004b). Table 5 summarizes the equivalent viscous damping and the equivalent stiffness.

5. Numerical simulation of shaking table test

Numerical simulation of shaking table test, as shown in Fig. 8, has been carried out using the SAP2000 Nonlinear Version. 2 bays of the steel frames are linked with beams elements assuming with pinned connections to represent the bolt and nut connections. Structural members are modeled based on the parameters determined from the tensile tests and the two-points loading tests. Members within each bay are rigidly connected continuously. The HDADS is modeled as a "link" element with constant damping coefficient (C_{eq}) and stiffness (K_{eq}) estimated based on the input frequency.

The damping coefficients, C_{eq} and K_{eq} of HDADS, are summarized in Table 5. Since the parameters vary with frequency, choosing the appropriate parameters is significant. The parameters are selected based on the dominant frequency of the time history input, since the response frequency will be close to the dominant frequency. For instant, dominant frequency of the compressed El Centro earthquake time history is 2.56 Hz. The dominant frequency of El Centro time history generated by the shaking table is in the range of 2.39 to 3.08 Hz. The dominant frequency at the 2nd floor and the 1st floor based on the accelerometers records are in the range of 2.44 to 4.05 Hz.

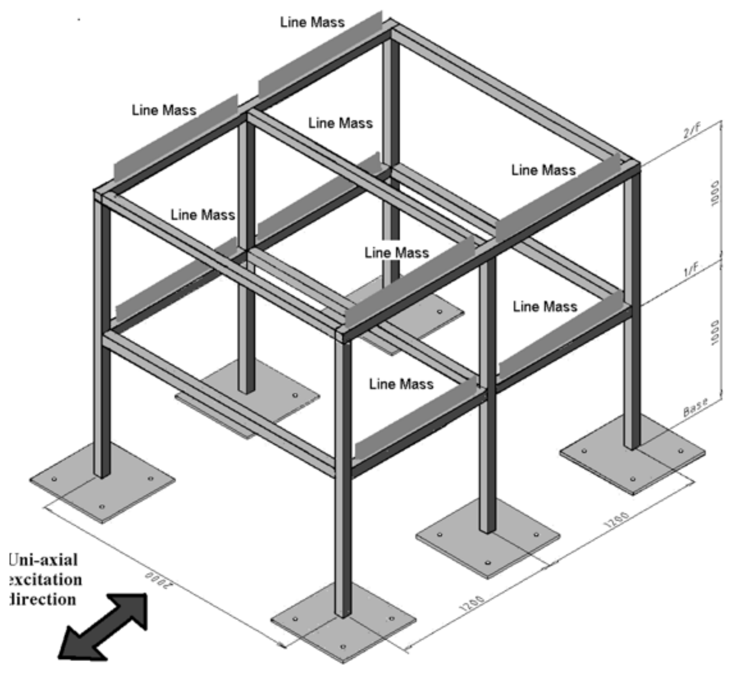

Fig. 8 Schematic drawing of numerical model of steel frame for shaking table test

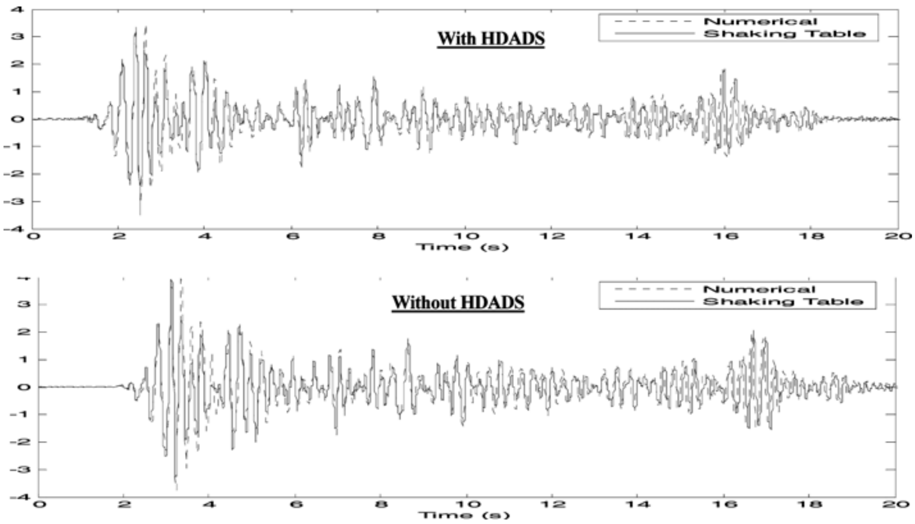

Fig. 9 Comparisons of acceleration at the 2nd floor (m/s^2) between numerical and experimental results

Therefore, in the numerical model of the HDADS, parameters at 3 Hz are used (C_{eq} and K_{eq} are 0.136 kNs/mm and 4.765 kN/mm respectively).

In comparing the first two natural frequencies obtained from the shaking table test and the numerical simulation, there are minor discrepancies between the two sets of results. Adjustment was carried out by varying the elastic modulus in the region of the welded connections between the members in each bay. The optimal sectional modulus was 18075 mm^3 (a reduction to 79% of the elastic modulus of members). This section modulus was adopted to all the welded connections.

A 0.625 ton/m line mass has been assigned to each frame as shown in Fig. 8. The ground accelerations used in the numerical simulation are the time histories obtained from the shaking table tests.

The interstory drifts at the 2nd floor of the experimental and numerical results are summarized in Table 6 and Table 7. The interstory drifts predicted by the numerical simulations are of acceptable accuracy. Structural performance of the steel frame can be predicted by the numerical models. Numerical simulation of the shaking table test subjected to sinusoidal excitation and earthquakes are carried out. The discrepancies of interstory drifts at the 2nd floor are below 16%. Fig. 9 shows time histories records of the acceleration at the 2nd floor subjected to the El Centro excitation obtained from experimental and numerical results. Reasonable results can be obtained by the numerical model.

6. Conclusions

A new energy dissipating system, the Hydraulic Displacement Amplification Damping System (HDADS), based on viscous fluid dampers with displacement amplification capability has been proposed in this paper. Shaking table tests of a 1/3 scale, 2 stories prototype steel frame have been carried out to verify the energy dissipating system. The system can be used to retrofit existing beam-column joints and can reduce the interstory drifts by 10 to 25% for moderate seismic earthquake. Numerical model of the HDADS has been developed. The numerical model has been used in numerical simulations of the shaking table tests. Results obtained from the numerical simulations are in good comparison with those obtained from experiments. The HDADS can provide possible means to prevent structural damage of beam-column joints against moderate seismic attacks.

Acknowledgements

The writers are grateful to the financial supports from the Research Grants Council of Hong Kong (RGC No: PolyU BQ-576). Valuable assistance from the Structural Dynamic Laboratory of the Hong Kong Polytechnic University is also gratefully acknowledged.

References

Berton, S. and Bolander, J.E. (2004), "Amplification system of supplemental damping devices in seismic application", *J. Struct. Eng.*, ASCE, **131**(6), 979-983.

Berton, S. (2001), "Displacement amplification method and apparatus for passive energy dissipation in seismic applications", *U.S. Pat.* No. 6,672,573 B2.

Booth, E. (1994), *Concrete Structure in Earthquake Regions: Design and Analysis*, Longman Scientific & Technical.

Chung, S.K.T. and Lam, S.S.E. (2004a), "Hydraulic displacement amplification system for energy dissipation", *2004 Annual Meeting: Networking of Young Earthquake Engineering Researchers and Professionals,* Honolulu, Hawaii, USA, July.

Chung, S.K.T. and Lam, S.S.E. (2004b), "Strengthening of reinforced concrete beam-column joints and columns by energy dissipation with hydraulic displacement amplification system", *Selected Papers on Earthquake Engineering and Engineering Seismology,* Harbin, China, August.

Code of Practice for Structural Use of Concrete 2004 (2004), Building Department, the HKSAR Government.

Constantinou, M. (1994), "Application of fluid viscous dampers to earthquake resistant design. research accomplishments, 1986-1994", *Buffalo: National Center for Earthquake Engineering Research*, 73-80.

Dhakal, R.P. and Pan, T.C. (2005), "Experimental study on the dynamic response of gravity-designed reinforced concrete connections", *Eng. Struct.,* Elsevier Science Ltd., **27**, 75-87.

GB50011-2001, National Standards of People Republic of China Code for Seismic Design of Building, Ministry of Construction.

Harris, H.G. and Sabnis, G.M. (1999), *Structural Modeling and Experimental Techniques*, 2nd Ed., CRC Press.

Jensen, V.H. (2000), "Seismic microzonation in Australia", *J. Asian Earth Sci.*, Elsevier Science Ltd., **18**, 3-15.

Lam, S.S.E. and Xu, Y.L. (2002), "Progress in earthquake resistant design of buildings in Hong Kong", *SEWC2002*, Yokohama Japan.

Lee, C.F., Ding, Y., Huang, R., Yu, Y., Guo, G., Chen, P. and Huang, X. (1996). *Seismic Hazard Analysis of the Hong Kong Region. GEO Report No. 65.* Civil Engineering Services Department, Hong Kong Government.

Lee, D. and Taylor, D.P. (2001), "Viscous Damper Development and Future Trends.", *Struct. Des. Tall Build.*, John Wiley & Sons, **10**, 311-320.

Ribakov, Y., Gluck, J. and Gluck, N. (2000), "Practical design of MDOF structures with supplemental viscous dampers using mechanical levers", *8th ASCE Specialty Conference on Probabilistic Mechanics and Structural Reliability.* ASCE.

Ribakov, Y. and Dancyoier, A.N. (2006), "High-efficiency amplifiers for viscous damped structures subjected to strong earthquakes", *Struct. Des. Tall Spec. Build.*, **15**(2), 221-232.

Ribakov, Y. and Reinhorn, A.M. (2003), "Design of amplified structural damping using optimal considerations", *J. Struct. Eng.*, ASCE, **129**(10), 1422-1427.

Robinson, W.H. and Cousins, W.J. (1987), “Recent developments in lead dampers for base-isolation”, *Proc. Pacific Conference Earthq. Eng.*, **2**, 279-283.

Shen, K.L. and Soong, T.T. (1996), “Design of energy dissipation devices based on concept of damage control”, *J. Struct. Eng.*, ASCE, **122**(1), 76-82.

Skinner, R.I., Kelly, J.M. and Heine, A.J. (1975), “Hysteresis dampers for earthquake-resistant structures”, *Earthq. Eng. Struct. Dyn.*, **3**(3), 287-296.

Soong, T.T. and Spencer, B.F. (2002), “Supplemental energy dissipation: state-of-the-art and state-of-the-practice”, *Eng. Struct.*, Elsevier Science Ltd., **24**(3), 243-259.

Steidel, R.F. (1989), *An Introduction to Mechanical Vibrations*, 3rd Ed., John Wiley & Sons.

Taylor, R.G. (1978), “Tapered steel energy dissipators for earthquake resistant structures”, *Bull. NZNSEE*, **11**(4), 282-294.

Tsopelas, P. and Constantinou, M.C. (1994), “Experimental and analytical study of a system consisting of sliding bearings and fluid restoring force/damping devices”, NCEER-94-0014, National Center for Earthquake Engineering Research.

Taylor, D.P. and Duflot, P. (2003), “Fluid viscous dampers to protect structures during earthquake”, *Fifth National Conference on Earthquake Engineering*, Istanbul, Turkey.